Journal of the Korean Society of Marine Environment & Safety
Research Paper
Vol. 23, No. 2, pp. 194-199, April 30, 2017, ISSN 1229-3431(Print) / ISSN 2287-3341(Online) https://doi.org/10.7837/kosomes.2017.23.2.194

# Behavioral Analysis of Silt Protectors in Seawater Using the Mass-Spring Model

Choon-Woo Lee* · Ok-Sam Kim**† · Hyun-Chool Shin** · Doo-Jin Hwang**

* Division of marine Production System management, Pukyong National University, 599-1 Daeyeon-Dong, Namgu, Busan, 48523, Korea
** Faculty of Marine Technology. Chonnam National University, 50 Daihak-ro, Yeosu, Chonnam, 59626, Korea

# 질량-스프링 모델을 이용한 해수 중 오탁방지막 거동해석

이춘우* · 김옥삼**† · 신현출** · 황두진**

* 부경대학교 수산과학대학 해양생산시스템관리학부, ** 전남대학교 수산해양대학 해양기술학부

**Abstract :** *When sea tide and wave velocity change, the behavior of silt protectors underwater changes, and a hydraulic force exceeding the anchor wave force is applied. In this study, the movement mechanism of a silt protector has been analyzed using the mass-spring method. The initial position of the silt protector was in the Jindo area near Gwangpo Port (742-1, Gyupori, Chongdo-myeon, Jindo-gun, Jeonnam, Korea). The tension required to exceed the holding power of the anchor was 0.05 m/s at 318 sec., 0.15 m/s at 77 sec., 0.25 m/s at 43 sec., and 0.3 m/s at 37 sec.. As the anchor started to move from the sea floor and the tide speed increased to 0.01 m/s, anchor movement start time shortened by an average of 11.2 sec.. Compared with when tide was the only affecting factor, the silt protector and anchor were found to have moved 19.7 % at 0.1 m/s, 7.6 % at 0.15 m/s, 5.8 % at 0.2 m/s, 4.3 % at 0.25 m/s and 2.8 % at 0.3 m/s, showing an increase. When wave effect was added to the tide, anchor movement started when the flow rate was slow 7.6 % of the time. With a high flow velocity, anchor movement started without any significant difference less than 4.3 % of the time. When tide speed exceeded 0.13 m/s and the direction of the waves matched, the silt protector was not able to perform due to collisions with surrounding sea structures. When installing a silt protector, the fluid flow situation and the silt protector situation must be carefully analyzed using the mass-spring method to apply the result found in this study.*

**Key Words :** *Silt protector, Mass-spring model, Behavior analysis in seawater, Tide, Waves*

**요 약 :** 오탁방지막이 바닷물 속에 설치되어 있을 때 조류와 파도가 변할 때 움직임과 앵커 파주력을 초과하는 유체력이 작용할 경우의 이동 메카니즘을 질량-스프링법으로 해석하였다. 설치 위치는 전남 진도군 임회면 굴포리 동령개 포구 해역이다. 앵커의 파주력을 초과하는 장력은 0.05 m/s에서는 318초 후에 도달하였고, 0.15 m/s에서는 77초, 0.25 m/s에서는 43초, 0.3 m/s에서는 37초 후에 앵커가 움직이기 시작하여, 조류 속도가 0.01 m/s로 증가함에 따라서 평균 11.2 초 정도, 앵커 이동시작 시간이 단축되고 있었다. 조류만 작용할 때와 파랑이 추가될 때의 차이점은 유속이 느릴 경우, 앵커의 이동이 시작되는 시간의 차이가 7.6 % 정도 발생하였으나, 유속이 빠른 경우는 4.3 % 미만으로 큰 차이가 없이 앵커 이동이 시작되는 것을 알 수 있었다. 조류 속도가 0.13 m/s를 초과하고 파도의 방향이 일치하면 주변의 해저 구조물과의 충돌로 인해 오탁방지막 성능이 정상적으로 작동하지 않을 수 있으니, 오탁방지막을 바다에 설치할 때 해수의 흐름 상황 등을 질량-스프링 방법으로 면밀하게 검토해야 한다.

**핵심용어 :** 오탁방지막, 질량-스프링 모델, 해수 중 거동해석, 조류, 파랑

## 1. Introduction

Use a silt protector to remove sludge and sludge deposited in the sea, rivers and lakes, or to prevent the spreading of suspended or polluted material during waterworks, such as dredging or slag discharging. It uses cylindrical float of polystyrene with superior buoyancy and silt curtain which is resistant to external force and filtration by using high tensile polyester synthetic fiber, consisting of a mooring rope and an anchor (Kee, 2002). The mooring line is connected to the anchor by a wire rope or a chain, and the sinker

* First Author : cwlee@pknu.ac.kr, 051-629-5891
† Corresponding Author : kos@jnu.ac.kr, 061-659-7153

at the bottom of the mound serves to reduce the rocking motion of the mound. There is a self-sustaining type that hangs a continuous cloth between a body and a heavy body, and supports a hanging system mooring to an anchor and a rope and a curtain type supporting the bottom of the sea. In order to obtain the effective tension in the mooring rope when installing the silt protector, the external force acting on the membrane and the body by waves and tidal currents based on the tide during high tide was calculated using the pseudo static load theory, rope tension (Hong et al., 2008). In this method, when the tide change width is large, the mooring rope that has been tightly installed on the basis of the tide during high tide is lowered due to the tidal drop and the tension is loosened so that the displacement is increased partially to restore the rope. This can lead to instability in the silt protector structure (Hong and Kim, 2002).

Therefore, when the silt protector installed in the sea is influenced by the tide and the wave and performs some movement and the hydraulic force exceeding the holding power of the fixed anchor acts, what kind of behavior and movement of the silt protector (Lee et al., 2005). As a concrete method, we used a mass-spring model that divides the silt protector structure in seawater into finite small elements and places the mass points at the midpoints of the divided elements, and analyzes the mass between the mass points as a spring-connected system.

## 2. Materials and methods

### 2.1 Installation condition of marine environment

The initial position of the silt protector is located at Jindo area near Gwangpo port (742-1, Gyupori, Chongdo-myeon, Jindo-gun, Jeonnam Korea) and Fig. 1.

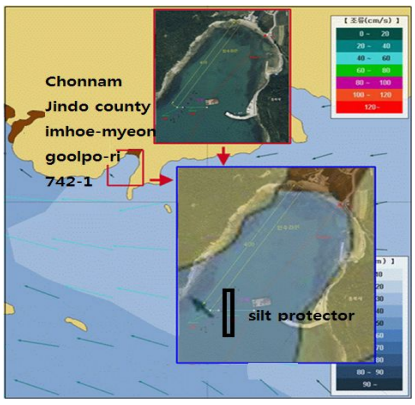


Fig. 1. Installation position of silt protector.

The installation state is connected to 6 of 20 m each, and the total length is 120 m. A styrofoam body with a total buoyancy of 600 kg is installed on the seawater surface for upward and downward development, and a sinker 8 mm in thickness is installed at an elevation of 8 m at high tide in the seawater. The weight of the silt protector in the air is 112 kg, the weight in the seawater is 97.35 kg, and the holding power per anchor is 486.7 kg. Two anchors are used at both ends of the silt protector, and nine 112 kg anchors, one at each of the middle widths, are fixed Fig. 2. The mooring rope connecting the anchor and the silt protector is made of polyethylene with a diameter of Φ28 mm, the length of both ends is 12 m, and the length of the intermediate mooring is 9 m. The mechanical properties and physical properties of the silt protector are shown in Table 1.

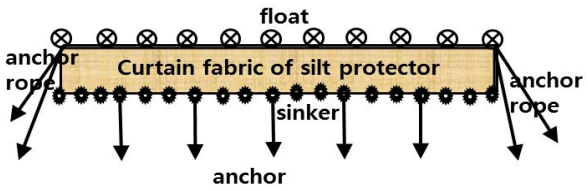


Fig. 2. Diagram of silt protector and anchors modeling of numerical analysis.

Table 1. Properties of silt protector

| Classify | Unit | Magnitude |
|---|---|---|
| Breaking strength | kg/in | ≥508×508 |
| Breaking elongation | % | 10～40 |
| Tearing strength | kg | ≥400×400 |
| Weight | g/m² | ≥1000 |
| Permeability | cm/sec | ≥a×10$^{-4}$ |
| Contraction ratio | % | ≤0.2×0.2 |
| Specific gravity | - | ≥1.0 |

The marine environmental data such as the tide and wave of the silt protector were used by the National Oceanographic Research Institute on September 1, 2010. The marine environment was analysis by two layers, tide and wave, which can be set direction and velocity, respectively, and operated in the same direction or arbitrary direction to analysis the behavior of structures such as silt protector in seawater. However, since the maritime environment and the maritime environment may be different from those of the maritime data and the silt protector, the flow rate range from 0.05

m/s to 0.3 m/s. Most of the waves reaching the coastal coast are assumed to be in a direction perpendicular to the coastline, approaching from the far sea at an angle of 60° to the direction of the tide. The applied wave is 0.7 m in wave height, 20 m in wave length, and the wave period was 8 seconds.

### 2.2 Analytical modeling of the behavior of the silt protector in seawater

The underwater flexible structure analysis program used in the analysis of the silt protector structure in seawater set the elastic structure as the mass-spring model (Lee et al., 2008). Structural deformation and motion in seawater due to external force were numerically calculated using the fourth-order Runge-Kutta method and expressed in 3-D form (Lee et al., 2010). In this case, it is assumed that all external forces such as mass, water resistance, lifting, buoyancy, and sinking force held by each element of the silt protector are concentrated on the mass point. The mass-spring model is applied to interpretation of the behavior of elastic structures such as net, rope and other floating structures in seawater, and its validity has already been verified Lee et al. (2010). This divides the structure in seawater into finite small elements, places the mass points at the center points of the divided elements, and interprets the mass between the mass points and the mass points as a connected system. The expansion and contraction of the silt protector fabric was also reflected by the elastic modulus of the spring considering the Young's modulus of the material. The float attached to the silt protector was input as the buoyancy of the material point placed at the corresponding position, and the chain used as the sinker was input as the sinking force to the mass point corresponding to the weight of water per unit length.

In order to reduce the calculation load, the silt protector was divided into a size of 0.5 m width × 0.5 m length, and the total was composed of 1,205 material points. In order to fix the silt protector to the seabed, the mooring rope connected to the anchor is divided into a certain length and the material points are arranged in the middle of each element Fig. 3, which are modeled by connecting springs between springs.

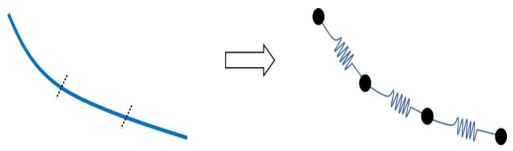

Fig. 3. Modeling of mooring rope for silt protector.

### 2.3 Motion equation of silt protector in seawater

The equations of motion for each mass point of silt protector in the sea are

$$(m+\triangle m)\ddot{q} = \overline{F_i}+\overline{F_e} \tag{1}$$

It can be expressed as a formula. Where $m$ is the mass of the mass point, $\Delta m$ is the added mass, $\ddot{q}$ is the acceleration vector, $\overline{F_i}$ is the internal force between the mass points, and $\overline{F_e}$ is the external force acting on the mass point. The added mass $\Delta m$, assuming that the external force does not act on the spring connecting the mass points, the external force works on the mass point only, and only the internal force due to the tension and compression of the spring acts

$$\triangle m = \rho_w V_n C_m \tag{2}$$

Where $\rho_w$ is the seawater density, $V_n$ is the volume of the mass point, and $C_m$ is the additional mass coefficient of equation (3).

$$C_m = 1 + \sin\alpha \tag{3}$$

In (3), $\alpha$ is the attack angle, and the internal force acting on the mass point is the force due to the tension and compressive force of the spring connecting the mass points. Internal force $\overline{F_i}$ acts on the silt protector and mooring rope only in tension direction and can be expressed as equation (4).

$$\overline{F_i} = -\hat{n}\frac{EA}{l^0}(|r|-l^0) \tag{4}$$

$E$ is the Young's modulus of the silt protector, $A$ is the effective area, $l^0$ is the original length of the spring, $\hat{n}$ is the unit vector of the spring position vector, and $|r|$ is the position vector corresponding to the spring. The spring constant value is calculated by taking the silt protector effective distance from the material and the distance between the material point and silt protector. The effective cross-sectional area of each element was taken into account the thickness of the silt curtain and the length of the cut surface. The apparent cross-sectional area and the effective Young 's modulus of the rope were set to 60 % of the original material Young' s modulus.

The external force $\overline{F_e}$ acting on the mass points distributed in the silt protector can be expressed by the equation (5) consisting of drag force $\overline{F_d}$, lift force $\overline{F_l}$, buoyancy and sinking force $\overline{F_b}$,

$$\overline{F_e} = \overline{F_d} + \overline{F_l} + \overline{F_b} \tag{5}$$

The drag $\overline{F_d}$ and lift $\overline{F_d}$ are shown in equations. (6) and (7).

$$\overline{F_d} = -1/2\,(C_d \rho_w S V^2 \widehat{n_v}) \tag{6}$$

$$\overline{F_l} = -1/2\,(C_l \rho_w S V^2 \widehat{n_l}) \tag{7}$$

Here, $C_d$ is a resistance coefficient, $S$ is a projected area of a material point, $V$ is a resultant velocity vector, $\widehat{n_v}$ is a unit vector for the resultant velocity vector, $C_l$ is a lift coefficient, and $\widehat{n_l}$ is a unit vector representing the direction of lift.

The resistance coefficient and the lift coefficient of the sea water structure for the silt protector were obtained from the test of the canvas for the development of the fishing boat and the following resistance coefficient $C_d$ and lift coefficient $C_l$ were used for the structure of the mooring rope.

$$C_d = (-1.34\sin\alpha^2 + 3.22\sin\alpha + 1.09)1.79Re^{-0.26} \tag{8}$$

$$C_l = -0.67\sin\alpha^3 + 0.13\sin\alpha^2 + 0.53\sin\alpha + 0.01 \tag{9}$$

The resistance coefficient and the lift coefficient change according to the attack angle as shown in Fig. 4. When the attack angle changes non-linearly, the accuracy is degraded. Therefore, the range of the attack angle is subdivided into a more linear equation.

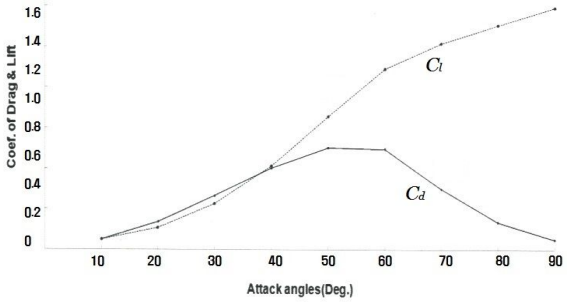


Fig. 4. Resistance coefficient and lift coefficient.

## 3. Results and discussion

### 3.1 Silt protector tide action

When the silt protector in the seawater receives a tide of 0.05 m/s to 0.3 m/s at right angles, the behavior is shown in Fig. 5. This is the side view of the silt protector movement according to the tide speed when 150 seconds passed after the tide. The silt protector started pumping even at a low flow rate of 0.05 m/s at the tide speed, and the displacement increased as the tide speed increased. If the tension on the mooring rope to which the anchor and silt protector are connected exceeds the anchor holding force, the anchor is programmed to move from that point onwards. When the anchor is moved in the sea floor, the tension of the anchor mooring rope increases as the silt protector is pushed by the resistance of the fluid force, which is increased after the tide exerts an external force on the silt protector. This tension exceeds the anchor holding force, the anchor is drawn and drawn. The anchor is pulled up, it is raised above the bottom of the sea, then it is stuck again, and if it exceeds the breaking force by the continuing acting force, it is pulled again and pulled again.

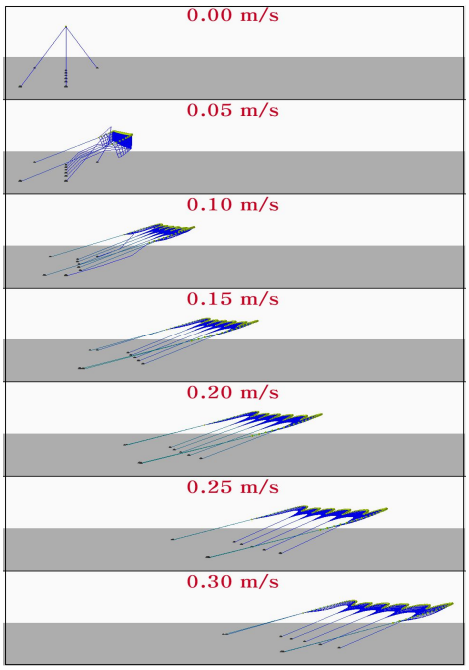


Fig. 5. Comparison of silt protector shape according to tide speed (150 sec.).

Fig. 6 shows that as the interpretation results, the faster the tide speed, the shorter the time the anchor starts moving. The x-axis in

this figure is the tide velocity, and the y-axis is the time (in seconds) at which the anchor begins to move, in logarithm coordinates. The anchor movement began at tide speeds of 0.05 m/s and more, although there was some time difference. As a result of the least squares analysis of the time at which the anchor started to move, $\sum(x_i - \overline{x})^2$ was 0.06. That is, the tension exceeding the holding force of the anchor reached 318 seconds at 0.05 m/s, 123 seconds at 0.1 m/s, 77 seconds at 0.15 m/s, 55 seconds at 0.2 m/s, 43 seconds at 0.25 m/s, the anchor began to move from the sea floor after 37 seconds at 0.3 m/s. In other words, if the tide speed increases to 0.01 m/s, the anchor movement start time is shortened by an average of 11.2 seconds.

300 seconds after the tide starts moving, the top view of the silt protector due to the tide velocity is shown in Fig. 7. In this figure, the silt protector anchor does not move at tide speed of 0.05 m/s when 300 seconds have passed since the tide starts to move, but it is 11.66 m at 0.1 m/s, 26.24 m at 0.15 m/S, and 56.17 m at 0.25 m/s and 71.07 m at 0.3 m/s, respectively. On average, this means that the anchor of the silt protector can move about 3 m from the sea floor at every 0.01 m/s increase in tide speed.

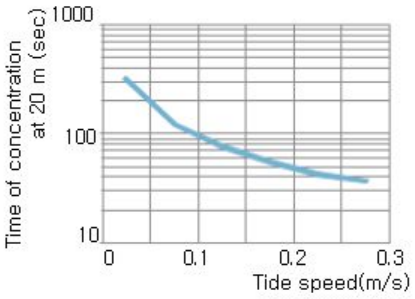


Fig. 6. Moving time of anchor according to tide speed.

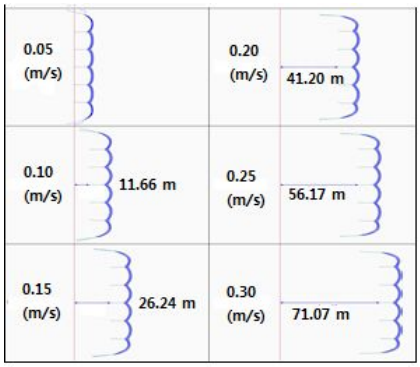


Fig. 7. Travel range of silt protector according to tide speed (300sec.).

### 3.2 Tide and wave work on silt protector

When the tide and wave act simultaneously on the silt protector, the analysis results are shown in Fig. 8 and Fig. 9. The wave added to the tide appears as a mixture of the displacement by the tide and the up and down movement by the wave. When the tide and wave interact with the silt protector, the silt protector and anchor are used at 13.96 m at tide speed of 0.1 m/s, 28.26 m at 0.15 m/s, 43.59 m at 0.2 m/s, 58.59 m at 0.25 m/s and 73.1 m at 0.3 m/s it was calculated to move from the sea floor.

Compared with when tide was the only function, at 0.1 m/s it was 2.3 m 19.7 %, at 0.15 m/s it was 2.0 m 7.6 %, at 0.2 m/s it is 2.4 m 5.8 %, at 0.25 m/s, 4.3 % at 2.4 m and when it is 0.3 m/s, it is 2.0 m and 2.8 % the moving distance of silt protector and anchor was increasing. The analysis of the difference between when tide only and when wave is added shows that when the flow rate is slower than 0.15 m/s, the difference in the time when the anchor starts moving is about 7.6 %, and when the flow rate was faster than 0.25 m/s, the anchor movement began without any significant difference of less than 4.3 %.

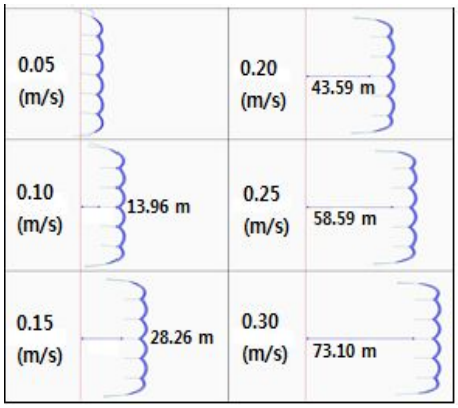


Fig. 8. Comparison of silt protector shape together tide and waves.

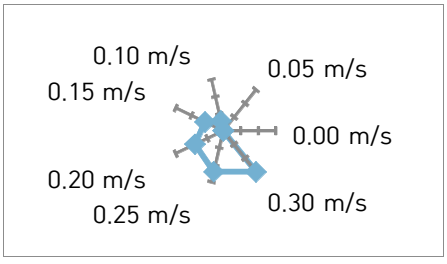


Fig. 9. Travel distance of anchor together tide and waves.

## 4. Conclusions

The flexible-structure analysis program in the seawater described by the mass-spring model was able to analysis underwater behavior, deformation and movement of the silt protector structure in seawater. The tension exceeding the holding power of the anchor is 318 sec at 0.05 m/s, at 0.15 m/s, 77 sec., 0.25 m/s at 43 sec, and 0.3 m/s at 37 sec. As the anchor started to move from the sea floor and the tide speed increased to 0.01 m/s the anchor movement start time was shortened by an average of 11.2 sec.. The moving distance of the anchor at sea is 11.66 m at 0.1 m/s, 41.2 m at 0.2 m/s and 71.07 m at 0.3 m/s and the average tide speed can move about 3 m for every 0.01 m/s increase.

The behavior when the wave was added to the tide was a mixture of displacement by the tide and up and down movement by the tide. It was 13.96 m at 0.1 m/s, 43.59 m at 0.2 m/s, and 73.19 at 0.3 m/s silt protector and anchor can move in the sea. Compared with when tide was the only function the silt protector and the anchor were found to be 19.7 % at 0.1 m/s, 7.6 % at 0.15 m/s, 5.8 % at 0.2 m/s, 4.3 % at 0.25 m/s and 2.8 % at 0.3 m/s moving distance is increasing. The difference between when tide and wave are added is that 7.6 % of the time when the anchor movement starts when the flow rate is slow. In the case of high flow velocity, the anchor movement started without any significant difference of less than 4.3 %.

If the tide speed exceeds 0.13 m/s and the direction of the wave is matched, the silt protector will not be able to perform due to collision with surrounding sea structures. Therefore, when installing the silt protector, the fluid flow situation and the silt protector situation must be carefully analyzed by the mass-spring method.

## References

[1] Hong, N. S., G. Y Kim and Y. K. Kang(2008), Three -dimensional numerical model for flow with silt protector, The Korean Society of Ocean Engineers, Vol. 22, No. 1, pp. 1-7.

[2] Hong, N. S. and J. Y. Kim(2002), Behavior of mooring line of silt protector according to the change of sea level, The Korean Society of Coastal Ocean Engineers, Vol 14, No. 4, pp. 232-239.

[3] Kee, S. T.(2002), Submerged membrane breakwaters Ⅰ: A rahmen type system composed of horizontal and vertical membranes, The Korean Society of Ocean Engineers, Vol. 16, No. 1, pp. 7-14.

[4] Lee, C. W., J. H. Lee, B. J. Cha, H. Y. Kim and J. H. Lee(2005), Physical modeling for underwater flexible systems dynamic simulation, Ocean Engineering, Vol. 32, pp. 331-347.

[5] Lee, C. W., J. H. Lee, M. Y. Choe and G. H. Lee(2010), Design and simulation tools for moored underwater flexible structures, Korea Journal Aqua. Sci., Vol. 43, pp. 159-168.

[6] Lee, J. H., L. Karlsen and C. W. Lee(2008), A method for improving the dynamic simulation efficiency of underwater flexible structures by implementing non-active points in modelling, ICES Journal of Marine Science, Vol. 65, No. 9, pp. 1552-1558.

Received : 2016. 12. 19.
Revised : 2017. 03. 18. (1st)
: 2017. 04. 03. (2nd)
Accepted : 2017. 04. 27.